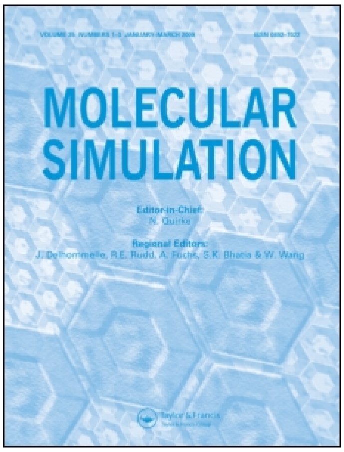

Molecular Simulation
Publication details, including instructions for authors and subscription information:
http://www.informaworld.com/smpp/title~content=t713644482

A Thermodynamic Investigation of Selenium Confined in Silicalite Zeolite

Christophe Bichara[a]; Jean-Yves Raty[b]; Roland Pellenq[a]
[a] Centre de Recherches sur les Mécanismes de la Croissance Cristalline, CNRS Case 913, Marseille Cedex 09, France [b] Département de Physique, Université de Liège, Sart Tilman, Belgique

To cite this Article Bichara, Christophe , Raty, Jean-Yves and Pellenq, Roland(2004) 'A Thermodynamic Investigation of Selenium Confined in Silicalite Zeolite', Molecular Simulation, 30: 9, 601 — 606

To link to this Article: DOI: 10.1080/08927020410001717218

URL: http://dx.doi.org/10.1080/08927020410001717218

Molecular Simulation, Vol. 30 (9), 10 August 2004, pp. 601–606

Taylor & Francis
Taylor & Francis Group

A Thermodynamic Investigation of Selenium Confined in Silicalite Zeolite

CHRISTOPHE BICHARA[a], JEAN-YVES RATY[b] and ROLAND PELLENQ[a,*]

[a]*Centre de Recherches sur les Mécanismes de la Croissance Cristalline, CNRS Case 913, Campus de Luminy, 13388, Marseille Cedex 09, France;* [b]*Département de Physique, Université de Liège, B5 B4000, Sart Tilman, Belgique*

(Received November 2003; In final form January 2004)

In this paper, we study the practical feasibility of selenium adsorption in silicalite-1 zeolite by performing Grand Canonical Monte Carlo (GCMC) simulations on a simulation box including the porous matrix and its outer surface. This work aims at gaining insight on the stability of semi-conductor wires in microporous materials. The simulations at two different temperatures show two distinct behaviors: adsorption occurs inside the pores at 200°C while solely on the external surface at 650°C. This indicates that adsorption inside the pore network can only proceed below the pseudo-wetting transition temperature that lies between 200 and 650°C. The existence of such transition temperature is thus crucial if one aims to produce nanowires from microporous materials by adsorption from a gas phase.

Keywords: Monte Carlo simulations; Microporous; Transition temperature; Semi-conductor

INTRODUCTION

Incorporating metallic or semi conducting guests in well organized micro- or mesoporous hosts is a possible route to synthesize novel materials with potentially interesting electronic or opto electronic properties. Selenium (Se) is an obvious choice for such an attempt since it is a semi conductor in solid and in the low temperature liquid states, and has low melting (221°C), boiling (685°C) and critical (1615°C, 385 bars [1,2]) points. According to the octet rule, selenium atoms prefer a 2-fold coordination and consequently, the stable solid and low temperature liquid phases display a chain structure. At high temperature and moderately high pressures (in the 1000–1600°C and 500–1500 bar ranges), the chains can break or connect via 1-fold of 3-fold defects that are the origin of the increase of electrical conductivity experimentally measured [3]. Tight binding [4] and *ab-initio* [5,6] simulations of the liquid have clarified the role of these defects to explain the unexpected correlation between the increase of conductivity and the decrease of the density and average coordination number experimentally observed [7].

It is thus very tempting to use the well defined channel or cage structure of a zeolite to try and control the electronic properties of the adsorbed Se phase, if ever adsorption is possible. The incorporation of Se in various microporous matrices has been reported in AlPO4-5 [8,9], a neutral zeolite with parallel channels of ≈ 7.3 Å diameter, in mordenite, cancrinite [10] and Y cage [11,12] zeolites.

In this work, we consider the possibility of incorporating Se in silicalite, a purely siliceous zeolite, which displays a complex structure of connected straight and zig-zag channels of 0.5 nm in diameter [13] that could impose 3-fold coordinated "defects" at the intersections possibly leading to new properties of the confined phase compared to the bulk (solid) phase in the same conditions of temperature and pressure. More precisely, we address the question of the feasibility of the experiment and try to answer the question of whether Se prefers to be adsorbed inside the zeolite or condensate outside.

COMPUTER SIMULATION TECHNIQUE

Since we focus here on neutral zeolites, the interaction of Se atoms with the walls is in the physisorption range. Details on the model for Se–Se and Se-silicalite interactions are given in the Appendix.

---

*Corresponding author. E-mail: xtof@crmcn.univ-mrs.fr

ISSN 0892-7022 print/ISSN 1029-0435 online © 2004 Taylor & Francis Ltd
DOI: 10.1080/08927020410001717218

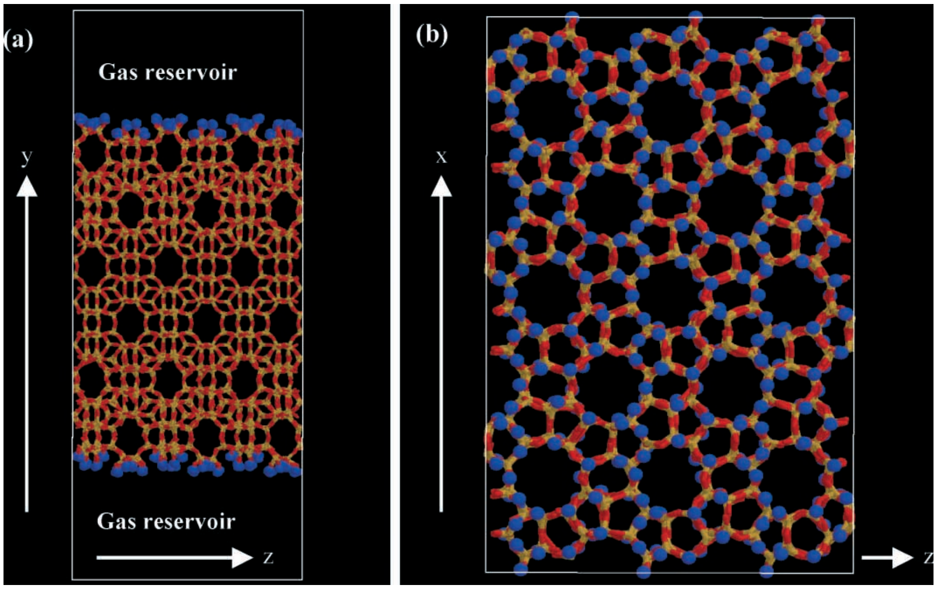

FIGURE 1 Two different views of the simulation box. The system dimensions are given in the text. Red, yellow and blue balls are oxygen, silicon and hydrogen atoms that cover the zeolite slab external surface.

We performed standard Grand Canonical Monte Carlo (GCMC) simulations [14] on a box containing a slab of silicalite zeolite and running into a gas reservoir in contact with the 010 face: the straight channels running along the y crystallographic direction are thus opened towards the gas tank. The total simulation cell thus contains a zeolite slab and a gas reservoir as shown in Fig. 1a, b. The total volume sampled in the simulation algorithm is $2a \times 4b \times 3c$ where $a = 1.992\,\mathrm{nm}$, $b = 2.007\,\mathrm{nm}$ and $c = 1.339\,\mathrm{nm}$; a, b and c being the silicalite unit cell dimensions along the x, y and z directions, respectively (note that the zeolite slab itself contains 12 $(= 2 \times 2 \times 3)$ orthorhombic unit cells of silicalite). On the external surface (in contact with the gas reservoir), all dangling oxygen bonds were saturated with hydrogen atoms in order to maintain electroneutrality (all hydrogen atoms were placed at a distance of 0.1 nm of the nearest unsaturated oxygen).

The GCMC procedure consists of randomly attempting atomic displacement, insertion and extraction steps inside the simulation cell volume at fixed chemical potential, temperature and volume. In our particular case, the chemical potential is referred to a fictitious ideal gas of Se *atoms* whereas the real Se vapor is a mixture of Se_n ($n = 4$, 12) ring *molecules*. This explains the very large values (typically of the order of $-2.0\,\mathrm{eV/atom}$, approximately the energy of Se–Se bond) of the chemical potential at which the adsorption takes place (see below). Without knowing the relation between the chemical potential and the pressure, one cannot decide whether or not the adsorption takes place at pressures below the saturating vapor pressure, in other words whether or not the adsorption from the gas phase is thermodynamically possible. Starting with a Se dimer randomly located, we gradually raised the chemical potential and recorded the average number of adsorbed atoms. The output of standard GCMC calculations is therefore the adsorption isotherm, i.e. the adsorbed quantity as a function of a chemical potential. Because the temperatures at which the calculations were carried out are relatively low compared to the cohesive energy of Se, the equilibration of the simulated samples is difficult and very long runs had to be performed. A minimum of 5×10^5 Monte Carlo macrosteps was performed, each macrostep consisting of randomly performing 1000 attempted displacements, 10 attempted insertion and 10 attempted removals of a Se atom.

Periodic boundary conditions are applied on the entire simulation cell in all directions. The adsorbate-zeolite energy (see below) is calculated following a grid-interpolation procedure in which the entire volume of the simulation cell (including the gas reservoir region, see Fig. 1a, b) is split into a collection of elementary volumes [15]. The adsorption potential energy is calculated at each corner of each elementary cube using the potential energy function defined below. During the course of the simulation, the adsorbate/matrix potential energy is obtained from a linear interpolation of the corresponding three-dimensional (3D) grid calculated prior to any GCMC run. The Se–zeolite grid data file contains 2×10^6 values $(100 \times 200 \times 100)$. The step between two consecutive grid points is less than 0.4 Å allowing a very good accuracy compared to a direct calculation looping over all matrix species, the grid-interpolation approach being very efficient in terms of CPU time.

RESULTS AND DISCUSSION

In a previous paper [16], we showed that the adsorption in an infinite crystal (with no external surface) seems to proceed via a first order transition mechanism, unexpected for a microporous system, often viewed as a paradigm of a one-dimensional system. The resulting adsorption isotherms obtained at two different temperatures (200 and 650°C), respectively are presented in Fig. 2. The ability of selenium to form chains that can possibly be connected via 3-fold defects at a reasonable energy cost, combined with the connected 3D structure of silicalite are the keys to understand this behavior. Note that the maximum loading is 46 Se atoms per silicalite unit cell.

Our goal is here to decide whether Se prefers to be adsorbed inside the zeolite or condensate outside. A first approach to this question is to calculate the adsorption/desorption isotherm of Se into silicalite using the standard GCMC procedure and to compare it with the condensation/evaporation isotherm of bulk selenium calculated under the same conditions. In the case of the condensation/evaporation isotherm for bulk selenium, there is obviously no interaction with the substrate and the corresponding energy is set to zero. The isotherms calculated at 650°C in a periodic box consisting of 12 unit cells of silicalite (infinite crystal, no outer surface) on the one hand or in a cubic box of 20 × 20 × 20 Å^3 on the other hand, are presented in Fig. 3. As expected for a first order transition, the adsorption/desorption process in the zeolite is not reversible and exhibits a quite large hysteresis loop. The condensation and evaporation branches for bulk selenium bracket the adsorption/desorption branches. Although it seems that the "average" chemical potential for adsorption/desorption lies slightly lower than the condensation/evaporation one, it is not possible to reach a firm conclusion from these calculations.

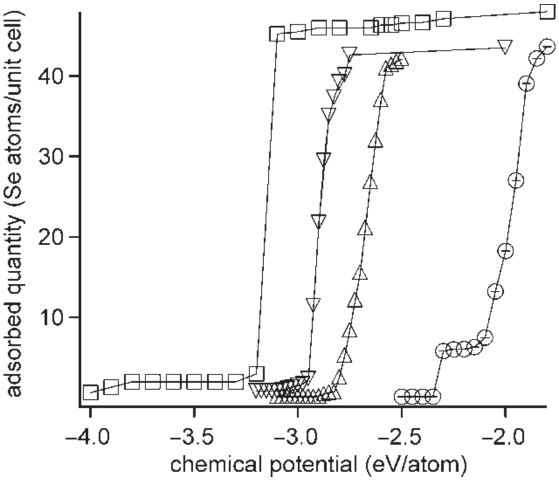

FIGURE 2 Adsorption isotherms of Se in silicalite (no external surface) at $T = 200$ and 650°C. Circles, adsorption at 200°C; squares, desorption at 200°C; upward triangles, adsorption at 650°C; downward triangles, desorption at 650°C.

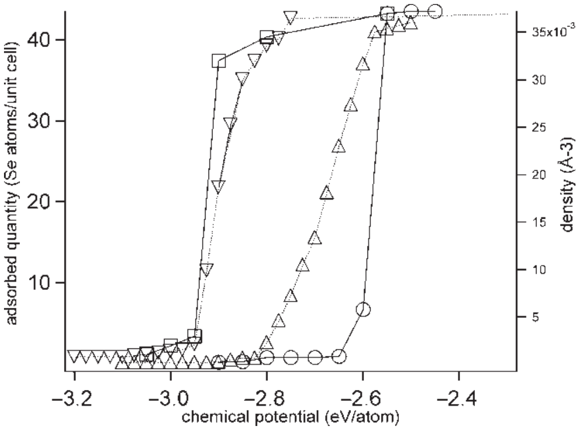

FIGURE 3 Condensation/evaporation (right y scale) and adsorption/desorption (left y scale) isotherms calculated at 650°C. Circles, bulk condensation; squares, bulk evaporation; upward triangles, adsorption; downward triangles, desorption.

An alternative possibility is to directly compute the equilibrium between the different phases. For this purpose, we now consider the simulation cell containing the zeolite slab and the gas reservoir as described above and consequently extend the active volume for the GCMC algorithm. In this case, during the GCMC run, Se atoms can either adsorb inside the microchannels of the zeolite or at its outer surface or condensate as a nano-droplet. Starting from the same initial configurations with two Se$_2$ dimers, randomly placed—one in a channel, the other one in the outer volume—we gradually increased the chemical potential from −2.50 to −2.10 eV/atom at 200°C and from −3.00 to 2.80 eV/atom at 650°C. It turns out that the system displays two completely different behaviors at these two temperatures. At low temperature, in agreement with our previous calculations [16], selenium adsorbs inside the pores at the same chemical potential value (−2.10 eV/atom). A snapshot of the last configuration is presented in Fig. 4, showing that a large majority of the 400 atoms is incorporated inside the zeolite, a minority of them remaining at the surface. As shown in Fig. 5, the situation is different at higher temperature. At a chemical potential value of −2.80 eV/atom, the adsorption only takes place on the outer surface of the crystal, with typically less than 10% of Se atoms inside the pores. Within the resolution of our calculation (increasing the chemical potential by steps of 0.025 eV/atom) and the finite number of Monte Carlo steps performed, this chemical potential value is slightly smaller than the chemical potential (−2.775 eV/atom) at which the adsorption began during our previous GCMC calculations ignoring the presence of the zeolite

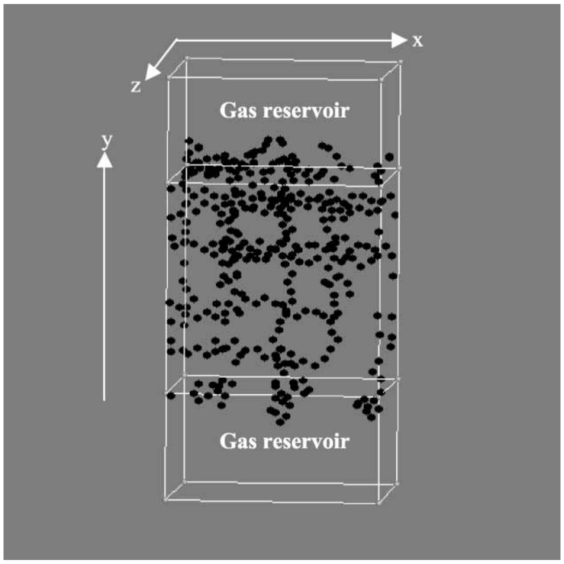

FIGURE 4 Typical configuration of a GCMC run at $T = 200°C$ and $\mu = -2.10\,eV/atom$. Most of the atoms are adsorbed inside the porous structure.

outer surface (see above). At this temperature, selenium prefers to wet the outer surface of the zeolite rather than being adsorbed inside the porous structure. This can easily be understood. At low temperature, the selenium chains maximize their interaction energy with the walls by occupying the porous volume. Since the pores are narrow (0.5 nm in diameter), their configurational entropy is low. By contrast, at higher temperature, the chains increase their configurational entropy by forming a wetting film on the outer surface of the zeolite grain.

A tentative sketch of the thermodynamic equilibria involved is presented in Fig. 6. From the theoretical point of view, our calculations imply that a "wetting" transition must take place between 200 and 650°C. The term "wetting" is somewhat improper since we have a transition from an adsorbed Se chain inside the pores to a molecular liquid film on the external surface; "wetting" being used to describe the surface first order transition between a molecular thick adsorbed film to a macroscopic thick film. Therefore, the term of pseudo-wetting is probably more appropriate. In this preliminary report, we did not investigate the intermediate temperature ranges, but we can see no reason why this transition should not take place. From the experimental point of view, our calculations indicate that incorporating Se in silicalite from the vapor phase at too high a temperature—which in some sense could be intuitive since a higher temperature means a higher vapor pressure of Se—will not be possible (i.e. it stabilizes a liquid phase on the outer surface). Other factors, such as the diffusion of Se in the pores, are of primary practical importance and are favorably influenced by an increase of the temperature, but the presence of a wetting transition sets an upper bound to any experimental procedure.

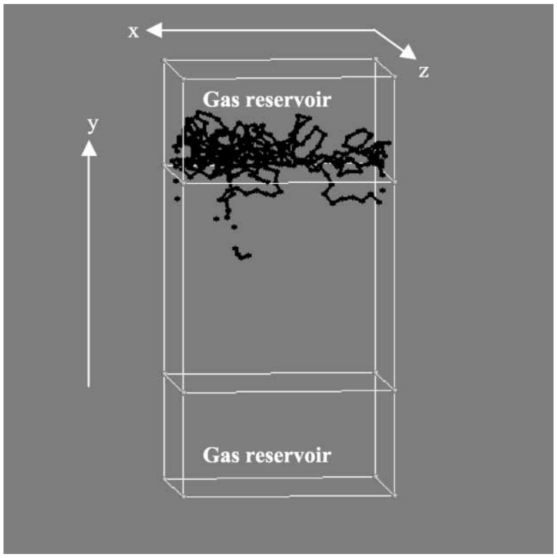

FIGURE 5 Typical configuration of a GCMC run at $T = 650°C$ and $\mu = -2.80\,eV/atom$. Most of the atoms are condensed on the external surface of the zeolite.

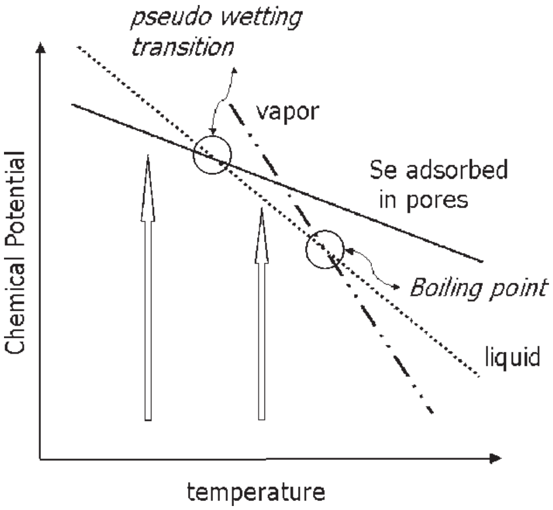

FIGURE 6 A tentative sketch of the phase equilibria of Se in silicalite. The two arrows indicate the temperatures at which the GCMC simulations were performed.

CONCLUSION

This paper reports a preliminary study of Se adsorption in zeolite silicalite. In particular, we investigate the role of the outer zeolite surface in the mechanism of adsorption by performing GCMC simulations. The simulation results at two different temperatures show two distinct behaviors: adsorption inside the pores at 200°C and condensation and pseudo-wetting on the external surface at 650°C. This indicates that adsorption can only proceed below a pseudo-wetting transition temperature (of the external zeolitic grain surface) that lies between 200 and 650°C. Since the mechanism involved (competition between an energy term dominant at low temperature and an entropic term that prevails at high temperature) is quite general, the existence of such pseudo-wetting temperature thus appears to be of crucial importance if one wants to practically incorporate selenium inside a microporous system with weak host–guest in the physisorption range.

APPENDIX

Selenium–zeolite Potential

The interaction of Se with Si, O and (surface) H atoms forming the zeolite structure is assumed to remain weak, in the physisorption energy range. In this work, we have used a TrAZ form of the original PN-type potential function as reported for adsorption of rare gases and nitrogen in silicalite-1 [17]. The PN-TrAZ potential function is based on the usual partition of the adsorption intermolecular energy restricted to two body terms only: it includes a dispersion interaction term, a repulsive short range contribution and an induction term. Three body dispersion (XYY) terms (where X is the adsorbate and Y an adsorbent species) can be obtained in principle from the same approach [18] but are neglected in the present study due to the large contrast between the Se–Se and the Se–zeolite interactions. In the TrAZ model, the adsorbate-surface energy (u_i) of a selenium gas atom at position i in the simulation box, is given by

$$u_i = \sum_{j \in \{\mathrm{O,Si,H}\}} \left[A_{ij} e^{-b_{ij} r_{ij}} - \sum_{n=3}^{5} f_{2n} \frac{C_{2n,ij}}{r_{ij}^{2n}} \right] - \frac{1}{2} \alpha E_i^2. \quad (1)$$

The sum runs over all atomic sites in the matrix that are oxygen and silicon atoms. The first term in the sum is a Born–Mayer term representing a two-body form of the short range repulsive energy due to finite compressibility of electron clouds when approaching the adsorbate at very short distance of the pore surface. There is one such term per pair of interacting species. The repulsive parameters (A_{ij} and b_{ij}) are obtained from mixing rules of like-atoms pairs (see below). The second term in the above equation is a multipolar expansion series of the dispersion interaction in the spirit of the quantum mechanical perturbation theory applied to intermolecular forces [19]. It has been shown that two (and three body) dispersion C_{2n} coefficients for isolated or in-condensed phase species can be obtained from the knowledge of the dipole polarizability and the effective number of polarizable electrons N_{eff} of all interacting species [17,19] which are closely related to partial charges that can be obtained from *ab initio* calculations. The f_{2n} terms in the above equation are damping functions of the form:

$$f_{2n} = 1 - \sum_{k=0}^{2n} \left[\frac{(b^{ij} r_{ij})^k}{k!} \right] \cdot e^{-b_{ij} r_{ij}} \quad (2)$$

The role of these damping functions is to avoid divergence of the dispersion interaction at short distance where the wave functions of the two species overlap (i.e. when the interacting species are at contact) [20]. They allow taking into account the possible electronic exchange which has a non zero probability at short distance even for two close shell structures, for each pair of interacting species, it is parametrized with the b_{ij} repulsive parameter. The damped dispersion multipolar expansion can be seen as a convenient way to make the perturbation theory valid at short inter-atomic separations. The last term in Eq. (1) is the induction interaction as written in the context of the quantum mechanical perturbation theory applied to intermolecular forces [19]. It represents an attractive energy arising from the coupling of the polarisable electronic cloud of the adsorbate of polarizability α at position i with the electric field E_i induced by the charges carried by framework species (O, Si and H) that result from the bonding process within the inorganic matrix itself. In total, one has to parametrize three different adsorbate/adsorbent-species potentials, the parameters are given in Table I. The assumption that bonding between the Se and zeolite does not involve chemisorption has been validated in the case of the Se/silicalite system by means of *ab initio* computer simulations [16]. The Se–zeolite interaction energy is typically around $-0.2\,\mathrm{eV/atom}$, that is order of magnitude is weaker than the stronger Se–Se covalent bonds and these two interactions are assumed to be independent and treated separately. All needed parameters for the dispersion interaction, multipolar development can be found from

TABLE I Se–silicalite potential parameters

	Se–O	*Se–H*	*Se–Si*
$C_6(E_h a_0^6)$	89.00	19.73	26.67
$C_8(E_h a_0^8)$	2273.1	457.5	625.9
$C_{10}(E_h a_0^{10})$	59893	–	–
A (E_h)	603.80	17.78	1206.6
b (a_0)	1.9070	1.980	1.981
		Zeolite partial charges	
$q(\mathrm{O}) = -1.0$	$q(\mathrm{H}) = +0.5$	$q(\mathrm{Si}) = +2.0$	
		Se properties	
Polarizabilities (a_0^3): $\alpha(\mathrm{Se}) = 24.5$		Number of polarizable electrons: $N_{\mathrm{eff}} = 5.63$	

known properties of interacting species. Repulsive parameters for like-pairs are taken from a previous work on the simulation of rare gases in silicalite [17], since atomic selenium has a van der Waals radius very close to that of krypton (2.0 Å; http://www.periodensystem.info/elemente/selen.htm and krypton.htm), we assumed that two selenium atoms will have the repulsive parameters of the Kr–Kr pair ($A_{\mathrm{Kr-Kr}} = 236.3E_h$ and $b_{\mathrm{Kr-Kr}} = 1.689a_0$; $1{\cdot}E_h = 27.211$ eV and $1{\cdot}a_0 = 0.529177$ Å).

Selenium–selenium Potential

The Se–Se interaction is described in a Tight Binding approximation which is a parameterized version of the Hückel theory. We use a minimal s, p_x, p_y and p_z atomic orbital basis set and a Slater Koster parameterization to build the Hamiltonian matrix describing the interaction. To avoid a time-consuming diagonalization of this matrix, we use the recursion method to calculate the local density of electronic states on each atom. We restrict the continued fraction expansion at the fourth moment's level which means that only first and second neighbors of each site are taken into account to calculate the band energy term. This approximation is quite crude but captures the quantum nature and the directionality of the bonding. In order to describe the weaker interchain or intermolecular bonds formed in the less dense phases of fluid selenium, a dispersion interaction term acting at distances beyond the tight binding cutoff radius is added [18], with suitable damping terms to smoothly switch from one to the other. As usual, a repulsive term prevents the collapse of the matter. The model for Se interaction then takes the general form:

$$E_{\mathrm{tot}} = E_{\mathrm{band}} + E_{VdW} + E_{\mathrm{rep}} \tag{3}$$

$$E_{\mathrm{tot}} = \sum_{\mathrm{sites}\, i}\left(\int_{-\infty}^{E_f} \mathrm{En}_i(E)\,\mathrm{d}E\right) - \sum_{i>j}\frac{C_6}{r_{ij}^6}F_2(r_{ij}) + \sum_{i>j} V_0\left(\frac{1}{r_{ij}}\right)^p F_1(r_{ij}) \tag{4}$$

where r_{ij} is the interatomic distance between sites i and j, $n_i(E)$ is the local density of state on site i, E_{f} is the Fermi level and C_6 is the attractive constant of the dispersion term (calculated from the polarizability of Se and a number of polarizable electrons [18]). $F_1(r_{ij})$ and $F_2(r_{ij})$ are damping functions. The values of V_0, p and the parameters defining the resonance integrals (not shown here) are given in Ref. [4]. This model was shown to accurately describe the structure of high temperature fluid selenium. The calculated thermodynamic properties (liquid–vapor equilibrium, critical point) of bulk Se were shown to be consistent with the experimental data in Ref. [21].

References

[1] Hosokawa, S. and Tamura, K. (1990) "Density measurement for fluid selenium by the X-ray absorption method", *J. Non-Cryst. Solids* **117/118**, 52–55.

[2] Hosokawa, S., Kuboi, T. and Tamura, K. (1997) "Density measurements for expanded fluid selenium up to the liquid vapour supercritical region by the X-ray absorption method", *Ber. Bunsenges. Phys. Chem.* **101**, 120–127.

[3] Hoshino, H., Schmutzler, R.W. and Hensel, F. (1976) "The high temperature vapour pressure curve and the critical point of liquid selenium", *Ber. Bunsenges. Phys. Chem.* **80**, 27–31.

[4] Raty, J.-Y., Saül, A., Gaspard, J.-P. and Bichara, C. (1999) "Structure of high-temperature fluid selenium", *Phys. Rev. B60* **4**, 2441–2448.

[5] Kresse, G., Kirchhoff, F. and Gillan, M.J. (1999) "Defects in liquid selenium", *Phys. Rev. B59* **5**, 3501–3513.

[6] Hoshino, K. and Shimojo, F. (1998) "The semiconductor-metal transition in fluid selenium studied by first-principles molecular dynamics simulation", *J. Phys.: Condens. Matt.* **10**, 11429–11438.

[7] Tamura, K. and Inui, M. (2001) "Structural changes and the metal-non-metal transition in supercritical fluids", *J. Phys.: Condens. Matter*, R337–R368, and references therein.

[8] Poborchii, V.V., Kolobov, A.V., Caro, J., Zhuravlev, V.V. and Tanaka, K. (1999) "Dynamics of single selenium chains confined in one-dimensional nanochannels of $\mathrm{AlPO_4}$-5: temperature dependencies of the first and second-order Raman spectra", *Phys. Rev. Lett.* **82**(9), 1955–1958.

[9] Sun, H.D., Tang, Z.K., Zhao, W.M. and Wong, G.K.L. (1997) "Temperature dependence of excitonic energy in isolated Se chains formed in channels of $\mathrm{AlPO_4}$-5 crystals", *Appl. Phys. Lett.* **71**(17), 2457–2459.

[10] Poborchii, V.V., Ivanova, M.S. and Ruvimov, S.S. (1994) "Polarized absorption and Raman spectra of 1-dimensional selenium chains in mordenite and cancrinite single crystals", In: Weitkamp, J., Karge, H.G., Pfeifer, H. and Hoelderich, W., eds, *Zeolites and related Materials: State of the Art 1994* (Elsevier) Studies in surface science and catalysis.

[11] Goldbach, A., Iton, L.E. and Saboungi, M.-L. (1997) "On the formation of isolated $\mathrm{Se_8}$ rings in zeolites", *Chem. Phys. Lett.* **281**, 69–73.

[12] Armand, P., Saboungi, M.-L., Price, D.L., Iton, L., Cramer, C. and Grimsditch, M. (1997) "Nanoclusters in zeolite", *Phys. Rev. Lett.* **79**(11), 2061–2064.

[13] Baerlocher, C., Meier, W.M. and Olson, D.H., *Atlas of Zeolite framework types* (Elsevier) fifth revised version, p 184.

[14] Nicholson, D. and Parsonage, N.G. (1982) *Computer Simulation and the Statistical Mechanics of Adsorption* (Academic Press, London).

[15] Pellenq, R.J.-M. and Nicholson, D. (1995) "Grand Ensemble Monte–Carlo simulation of simple molecules adsorbed in silicalite-1 zeolite", *Langmuir* **11**, 1626–1635.

[16] Bichara, C., Raty, J.-Y. and Pellenq, R.J.-M. (2002) "Adsorption of selenium wires in silicalite zeolite: a first order transition in a microporous system", *Phys. Rev. Lett.* **89**(1), 016101.

[17] Pellenq, R.J.-M. and Nicholson, D. (1994) "Potential function for rare gases interacting with silicalite-1 zeolite", *J. Phys. Chem.* **98**, 13339.

[18] Pellenq, R.J.-M. and Nicholson, D. (1998) "A simple method for calculating dispersion coefficients for isolated and condensed-phase species", *Mol. Phys.* **95**, 549.

[19] Stone, A. (1996) *The Theory of Intermolecular Forces* (Clarendon Press, Oxford).

[20] Tang, K.T. and Toennies, J.P. (1984) "An improved simple model for the van der Waals potential based on universal damping functions for the dispersion coefficients", *J. Chem. Phys.* **80**, 3726.

[21] Bichara, C., Gaspard, J.-P. and Raty, J.-Y. (2002) "Computer simulation of liquid semiconductors", *J. Non-Cryst. Solids* **312–314**, 341–348.